THE JOURNAL OF BIOLOGICAL CHEMISTRY VOL. 289, NO. 17, pp. 11704–11714, April 25, 2014

The Absence of Core Fucose Up-regulates GnT-III and Wnt Target Genes

*A POSSIBLE MECHANISM FOR AN ADAPTIVE RESPONSE IN TERMS OF GLYCAN FUNCTION**

Received for publication, July 16, 2013, and in revised form, February 28, 2014 Published, JBC Papers in Press, March 10, 2014, DOI 10.1074/jbc.M113.502542

Ayako Kurimoto[‡], Shinobu Kitazume[‡], Yasuhiko Kizuka[‡], Kazuki Nakajima[‡], Ritsuko Oka[‡], Reiko Fujinawa[‡], Hiroaki Korekane[‡], Yoshiki Yamaguchi[§], Yoshinao Wada[¶], and Naoyuki Taniguchi[‡1]

From the [‡]Disease Glycomic Team and [§]Structural Glycobiology Team, RIKEN Global Research Cluster, RIKEN-Max Planck Joint Research Center, RIKEN, 2-1 Hirosawa, Wako, Saitama 351-0198 and the [¶]Research Institute, Osaka Medical Center for Maternal and Child Health, Izumi, Osaka, 840 Murodo-cho, Izumi, Osaka 594-1101, Japan

Background: Little is known about how loss of a given glycan causes adaptive regulation of other glycosylation.
Results: Deficiency in core α1,6-fucose specifically up-regulates bisecting GlcNAc by enhanced gene expression of a biosynthetic enzyme GnT-III.
Conclusion: Wnt signaling pathway regulates the expression of GnT-III.
Significance: Wnt-mediated GnT-III up-regulation may be an adaptive response to the loss of core fucose.

Glycans play key roles in a variety of protein functions under normal and pathological conditions, but several glycosyltransferase-deficient mice exhibit no or only mild phenotypes due to redundancy or compensation of glycan functions. However, we have only a limited understanding of the underlying mechanism for these observations. Our previous studies indicated that 70% of Fut8-deficient (*Fut8*$^{-/-}$) mice that lack core fucose structure die within 3 days after birth, but the remainder survive for up to several weeks although they show growth retardation as well as emphysema. In this study, we show that, in mouse embryonic fibroblasts (MEFs) from *Fut8*$^{-/-}$ mice, another *N*-glycan branching structure, bisecting GlcNAc, is specifically up-regulated by enhanced gene expression of the responsible enzyme *N*-acetylglucosaminyltransferase III (GnT-III). As candidate target glycoproteins for bisecting GlcNAc modification, we confirmed that level of bisecting GlcNAc on β1-integrin and N-cadherin was increased in *Fut8*$^{-/-}$ MEFs. Moreover using mass spectrometry, glycan analysis of IgG_1 in *Fut8*$^{-/-}$ mouse serum demonstrated that bisecting GlcNAc contents were also increased by Fut8 deficiency *in vivo*. As an underlying mechanism, we found that in *Fut8*$^{-/-}$ MEFs Wnt/β-catenin signaling is up-regulated, and an inhibitor against Wnt signaling was found to abrogate GnT-III expression, indicating that Wnt/β-catenin is involved in GnT-III up-regulation. Furthermore, various oxidative stress-related genes were also increased in *Fut8*$^{-/-}$ MEFs. These data suggest that *Fut8*$^{-/-}$ mice adapted to oxidative stress, both *ex vivo* and *in vivo*, by inducing various genes including GnT-III, which may compensate for the loss of core fucose functions.

There are over 180 glycosyltransferase genes in mammals, and limited kinds of glycosyltransferase knock-out (KO) mice show severe phenotypic abnormality, demonstrating essential roles of glycans for various physiological functions. However, most of glycosyltransferase KO mice show no or very mild phenotypic changes (1). This suggests that there exist some mechanisms of the redundancy of glycosyltransferases and compensation for the lack of the product of glycosyltransferase(s). In fact, several family members of glycosyltransferase are known to be functionally redundant (1), but so far little is known about the mechanisms by which mammals can adapt to the loss of a given glycan.

α1,6-Fucosyltransferase (Fut8)[2] catalyzes the transfer of an α1,6-fucose residue from GDP-fucose to the innermost GlcNAc residue of glycans on glycoproteins (2). Purification and cDNA cloning of Fut8 from human and porcine were carried out by our group (3, 4). This core fucosylation is generally recognized to be physiologically important glycosylation by the fact that *Fut8*$^{-/-}$ mice show a semilethal phenotype, which includes severe growth retardation and emphysema-like lung destruction (5). These abnormalities are mainly caused by dysfunction due to the conformational changes of the receptors such as TGF-β1 and EGF receptors (6, 7).

Removal of the core fucose from human IgG_1 results in a significant enhancement in antibody-dependent cellular cytotoxicity (8), caused by the stronger binding of IgG_1 to Fcγ

* This work was supported by RIKEN (the Systems Glycobiology Research project) (to N. T.), Grant-in-Aid for Scientific Research (A) 20249018 (to N. T.), and the global Certificate of Eligibility (COE) program (to N. T.) from the Ministry of Education, Culture, Sports, Science and Technology of Japan.

The microarray data have been deposited to the National Center for Biotechnology Information (NCBI) Gene Expression Omnibus (GEO; www.ncbi.nlm.nih.gov/geo) under GEO accession number GSE49336.

[1] To whom correspondence should be addressed: Disease Glycomics Team, Systems Glycobiology Research Group, RIKEN-Max Planck Joint Research Center for Systems Chemical Biology, Global Research Cluster, RIKEN, 2-1 Hirosawa, Wako 351-0198, Saitama, Japan. Tel.: 81-48-467-8094; Fax: 81-48-467-8104; E-mail: tani52@wd5.so-net.ne.jp.

[2] The abbreviations used are: Fut8, α1,6-fucosyltransferase; MEF, mouse embryonic fibroblast; GnT-III, *N*-acetylglucosaminyltransferase III; GnT-IV, *N*-acetylglucosaminyltransferase-IV; GnT-V, *N*-acetylglucosaminyltransferase V; E4-PHA, phytohemagglutinin-E4; L4-PHA, phytohemagglutinin-L4; AAL, *Aleuria aurantia* lectin; LEF1, lymphoid enhancer-binding factor1; DMSO, dimethyl sulfoxide; FAM, 6-carboxyfluorescein; TAMRA, 6-carboxytetramethylrhodamine; Hex, hexose.

receptor IIIa (FcγR IIIa) (9), whereas several studies also reported that high content of IgG_1 modified with bisecting GlcNAc, synthesized by GnT-III, leads to higher antibody-dependent cellular cytotoxicity activity (10, 11). In addition, cellular functions of many glycoproteins, such as cadherins and integrins, are regulated by bisecting GlcNAc (12–17).

Our group has been extensively studying the role of core fucose and bisecting GlcNAc as modifiers/regulators of the *N*-glycan (18–20). Although the substrate specificity of Fut8 has been extensively studied, the issue of how the lack of a core fucose would affect the overall *N*-glycan structure remains unknown. Substrate specificity of Fut8 is strictly regulated because the addition of Gal or bisecting GlcNAc to *N*-glycans destroys their ability to serve as a substrate for Fut8 (21, 22). Replica-exchange molecular dynamics simulations of complex-type biantennary glycans revealed that the number of the major conformers is reduced upon the introduction of bisecting GlcNAc and/or core fucose (23). It was proposed that such conformer selection by bisecting GlcNAc and core fucose (23) may regulate the binding affinity of a target protein to which core fucose is added, an example of which is the TGF-β1 receptor. However, interplay of expression/function between core fucose and bisecting GlcNAc has not been studied well so far.

In this study, we initially adopted a glycomic approach to compare the *N*-glycan structures between $Fut8^{+/+}$ and $Fut8^{-/-}$ MEFs. The findings indicate that overall *N*-glycan structures are altered in $Fut8^{-/-}$ MEFs. Especially, bisected *N*-glycan was markedly increased in $Fut8^{-/-}$ MEFs. We then found that mRNA expression of GnT-III is increased by about 3-fold together with Wnt/β-catenin signaling as well as oxidative stress related genes, suggesting that an adaptive response may occur in $Fut8^{-/-}$ mice to compensate for the absence of core fucose.

EXPERIMENTAL PROCEDURES

Cell Culture—Mouse embryonic fibroblasts (MEFs) derived from wild-type and $Fut8^{-/-}$ mice (C57BL/6 genetic background) were established as described in a previous study (5). MEFs were cultured in DMEM supplemented with 10% FBS and penicillin and streptomycin at 37 °C in 5% CO_2-humidified atmosphere. In the case of the Wnt inhibition experiment, the media were supplemented with either DMSO or IWP-2 (final 15 μM) (Wako Pure Chemical), and the media were changed every 24 h for 3 days.

Lectin Blotting—Each sample was separated on SDS-PAGE and transferred to a nitrocellulose membrane. The membrane was blocked with 1% BSA in TBS-T for 30 min and incubated for 1 h with HRP-phytohemagglutinin-L4 (L4-PHA) or HRP-phytohemagglutinin-E4 (E4-PHA) lectin, which were used at 1/1000 dilution. After washing with TBS-0.1% Tween 20 (TBS-T), lectin reactive proteins were detected using a 3-fold diluted SuperSignal West Dura extended duration substrate (Thermo Scientific).

In the case of biotinylated *Aleuria aurantia* lectin (AAL) (1/1000 dilution), the membrane was blocked with TBS-T for 30 min. Lectin reactive proteins were detected using a VECTASTAIN ABC kit (Vector Laboratories), and the blots were developed according to the manufacturer's instructions.

Glycosyltransferase Assay—MEFs, grown on 10-cm dishes to full confluence, were suspended with 60–100 μl of 10 mM Tris-HCl (pH 7.4), 0.25 M sucrose, and proteinase inhibitors and then sonicated for 5 min on ice-chilled water bath with the Bioruptor sonicator (Cosmo Bio). The lysates were centrifuged at 12,000 × *g* for 5 min. The protein contents of the resulting supernatants were determined using a BCA protein assay (Thermo Scientific). Detailed procedures were reported in a previous study (24). The enzyme activities of Fut8, GnT-III, IV and V were determined using a pyridylamino-labeled oligosaccharide (TaKaRa pyridylamino-sugar chain 012) as an acceptor substrate. The resulting 3 μl of cell lysates, 5 μl of reaction buffer (200 mM MOPS-NaOH (pH 7.0), 20 mM $MnCl_2$, 400 mM GlcNAc, 1% Triton X-100, 2 mg/ml BSA), 1 μl of 0.1 mM acceptor substrate, and 1 μl of 400 mM UDP-GlcNAc were incubated at 37 °C for 4 h. The reaction was stopped by boiling for 3 min after adding 40 μl of water followed by centrifugation at 20,000 × *g* for 5 min. Resulting supernatant (10 μl) was used for assay of Fut8 and GnT activities by HPLC as described previously (25).

N-Glycan Digestions—$Fut8^{+/+}$ and $Fut8^{-/-}$ MEFs (5×10^7 cells) were washed three times with ice-cold PBS. The cell pellets were lysed with 500 μl of 1% Triton X-100 in PBS containing a protease inhibitor cocktail. After centrifugation of the cell suspension at 10,000 × *g* for 10 min, the supernatant was mixed with 3 volumes of ice-cold 95% ethanol and then incubated at −80 °C for 3 h. The suspension was centrifuged at 15,000 × *g* for 10 min. The precipitation was first reduced (10 mM DTT for 30 min at room temperature in 50 mM NH_4HCO_3) and then alkylated in the dark (20 mM 2-iodoacetamide at room temperature for 30 min). This was followed by digestion with 25 μl of 2 mg/ml trypsin and chymotrypsin (Nacalai Tesque) in 50 mM NH_4HCO_3 overnight at 37 °C. The digested mixtures were boiled for 5 min followed by incubating with 5 μl of peptide *N*-glycosidase F (New England Biolabs) for 18 h at 37 °C. After removing the insoluble materials by centrifugation, the supernatants were lyophilized. The digested samples were redissolved in 250 μl of 5% (v/v) acetic acid for solid-phase extraction with Oasis HLB extraction cartridges. Released oligosaccharide was recovered by collecting the flow-through, which is at least 5 ml of 5% acetic acid. The released glycans were lyophilized. The amount of obtained glycans was quantified by the phenol-sulfuric acid method (26).

Permethylation of N-Glycan—To enhance the sensitivity of *N*-glycan analysis by mass spectrometry, permethylation of *N*-glycans was performed by the NaOH/DMSO slurry method (27). To prepare the NaOH slurry, small beads of NaOH (50 mg, Fluka) were mixed with 250 μl of DMSO (∞Pure, Wako Pure Chemical) in an agate mortar. The slurry was added to the lyophilized 1 mg of *N*-glycan sample and vigorously agitated with 50 μl of iodomethane (Wako Pure Chemical) for 30 min. To stop the reaction, 1 ml of ice-cold water was added to the reaction mixture, and the resulting mixture was applied to a prewashed Oasis HLB column (Waters), followed by 1 ml of acetonitrile and dried under a N_2 stream. Obtained permethylated glycan was analyzed using Bruker Ultraflex MALDI mass spectrometry.

Permethylated Glycan Analysis by MALDI-TOF-MS—The permethylated oligosaccharides were dissolved in methanol and spotted on an MTP AnchorChip 400/384 T F plate with 10 mg/ml 2,5-dihydroxybenzoic acid and 5-methoxysalicylic acid (SDHB, Bruker) dissolved in a 0.1% (v/v) TFA and acetonitrile solution (2:1) for measurement. MS spectra were acquired on an Ultraflex MALDI-TOF/TOF (Bruker). MS^n spectra were recorded on an AXIMA-QIT TOF-MS (Shimadzu Biotech). Sample and 10 mg/ml 2,3-dihydroxybenzoic acid in 0.1% TFA and acetonitrile (3:2) (Shimadzu) were applied on a μFocus MALDI plate magnetic holder for Shimadzu. The measurements were carried out in the positive ion mode. The mass spectra acquired by at least 200 laser shots were accumulated, and the measurement was repeated at least three times. The peak height of the $[M+Na]^+$ ions was measured for relative semiquantitation at MS analysis. The fragmentation nomenclature for oligosaccharide by Domon and Costello (28) was used for MS^n analysis.

Immunoprecipitation—The cell lysates (adjusted to be less than 1 mg/ml of protein concentration) prepared from $Fut8^{+/+}$, $Fut8^{-/-}$, and reintroduced MEFs were incubated with 3 μg of a purified anti-mouse/rat CD29 (β1-integrin) antibody (BioLegend) at 4 °C overnight. Membrane fractions (100–200 μg) were incubated with 3 μg of anti-β1-integrin antibody (BD Biosciences) at 4 °C overnight. Membrane fractions in TBS-1% Triton X-100 were incubated with anti-N-cadherin antibody (Abcam). For precipitation, 20 μl of 50% slurry of protein G-agarose (GE Healthcare) was added and incubated at 4 °C for 30 min. The precipitates were washed three times with PBS and analyzed by Western blotting.

Western Blotting—MEF lysates were prepared in 1% Triton X-100 in PBS containing a protease inhibitor cocktail (Roche Applied Science). Protein concentration was determined using a BCA protein assay. The whole cell lysates (40 μg/lane) or immunoprecipitated samples were subjected to SDS-PAGE using 4–20%, 5–20% gradient or 5% gel, and transferred to nitrocellulose membranes. After the membranes were blocked in 5% nonfat dried milk in TBS containing 0.1% Tween 20, the membranes were incubated with primary antibodies. HRP-conjugated donkey anti-mouse IgG was used as the secondary antibodies, and a chemiluminescent substrate, SuperSignal West Dura extended duration substrate (Thermo Fisher Scientific), was used for detection. The detected bands were scanned using a Luminoimage analyzer LAS-1000 (Fujifilm). The following antibodies were used in this study: β1-integrin (BioLegend), N-cadherin (BD Biosciences), catenin (BD Biosciences), phospho-β-catenin (phospho-Ser-33/Ser-37/Thr-41) (Cell Signaling), phospho-β-catenin (phospho-Ser-552) (Cell Signaling), phospho-β-catenin (phospho-Ser-675) (Cell Signaling), lymphoid enhancer-binding factor 1 (LEF1), histone H3 (Cell Signaling), syntaxin 6 (BD Biosciences) and β-actin (Sigma-Aldrich). The antibodies were used at 1/1000 dilution.

Purification of IgG_1 from Mouse Serum and Analysis by MALDI-TOF MS—Serum from $Fut8^{+/+}$ and $Fut8^{-/-}$ mice (16-week-old male and female mice, ICR genetic background) were a generous gift from Dr. Jianguo Gu (Tohoku Pharmaceutical University). The amount of IgG was determined using a mouse IgG ELISA kit (Roche Applied Science). Mouse serum, containing 100–200 μg of IgG, was diluted 10-fold with phosphate buffer (pH 7.0). The mouse serum was purified on a protein G-Sepharose column (300 μl). After washing the column with phosphate buffer (pH 7.0), mouse IgG was eluted with IgG elution buffer (Thermo Scientific) followed by neutralization with 1 M Tris-HCl (pH 9.0). The freeze-dried eluate was dissolved in 400 μl of a solution of 6 M guanidine and 0.25 M Tris-HCl, pH 8.0, reduced with 0.13 M dithiothreitol at 56 °C for 1 h and then alkylated with 0.22 M iodoacetamide for 30 min at room temperature in the dark. The reactant was applied to a NAP5 column (GE Healthcare) equilibrated with 0.05 N HCl, eluted with 1 ml of 0.05 N HCl as reported previously (29–31). Briefly, the eluate was digested with trypsin and lysylendopeptidase (Wako Pure Chemical) at 37 °C for 18 h. Obtained glycopeptides were purified using Sepharose CL4B (GE Healthcare) in *n*-butanol/ethanol/water (4:1:1) and 50% aqueous ethanol. The aqueous ethanol fraction was dried using a SpeedVac, and the glycopeptide samples were mixed with 10 mg/ml of 2,3-dihydroxybenzoic acid, used as a matrix, which was prepared by dissolving 50% (v/v) acetonitrile solution. The glycopeptide analysis was accomplished using a Voyager DE Pro MALDI-TOF mass spectrometer (Applied Biosystems). The measurements were carried out in positive ion and linear mode.

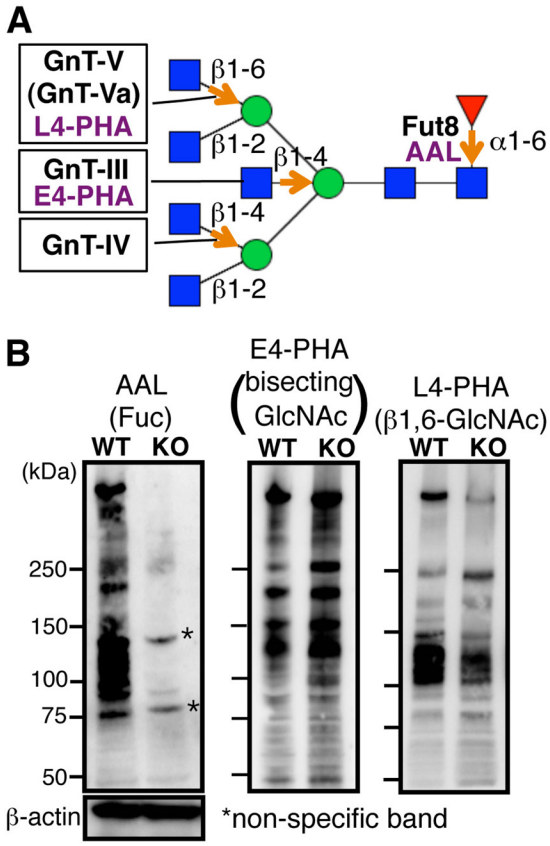

FIGURE 1. **The level of bisecting GlcNAc was increased in $Fut8^{-/-}$ MEFs.** *A*, symbolic representations of *N*-glycan and responsible glycosyltransferase, such as GnT-III, GnT-IV, GnT-V, and Fut8, are shown. Lectins, such as L4-PHA, E4-PHA, and AAL, preferentially recognized the indicated sites. *B*, lectin blot analysis of the cell lysates (40 μg of proteins) prepared from $Fut8^{+/+}$ and $Fut8^{-/-}$ MEFs were performed with AAL, E4-PHA, and L4-PHA. Western blot analysis with anti-β actin was also performed as an internal standard.

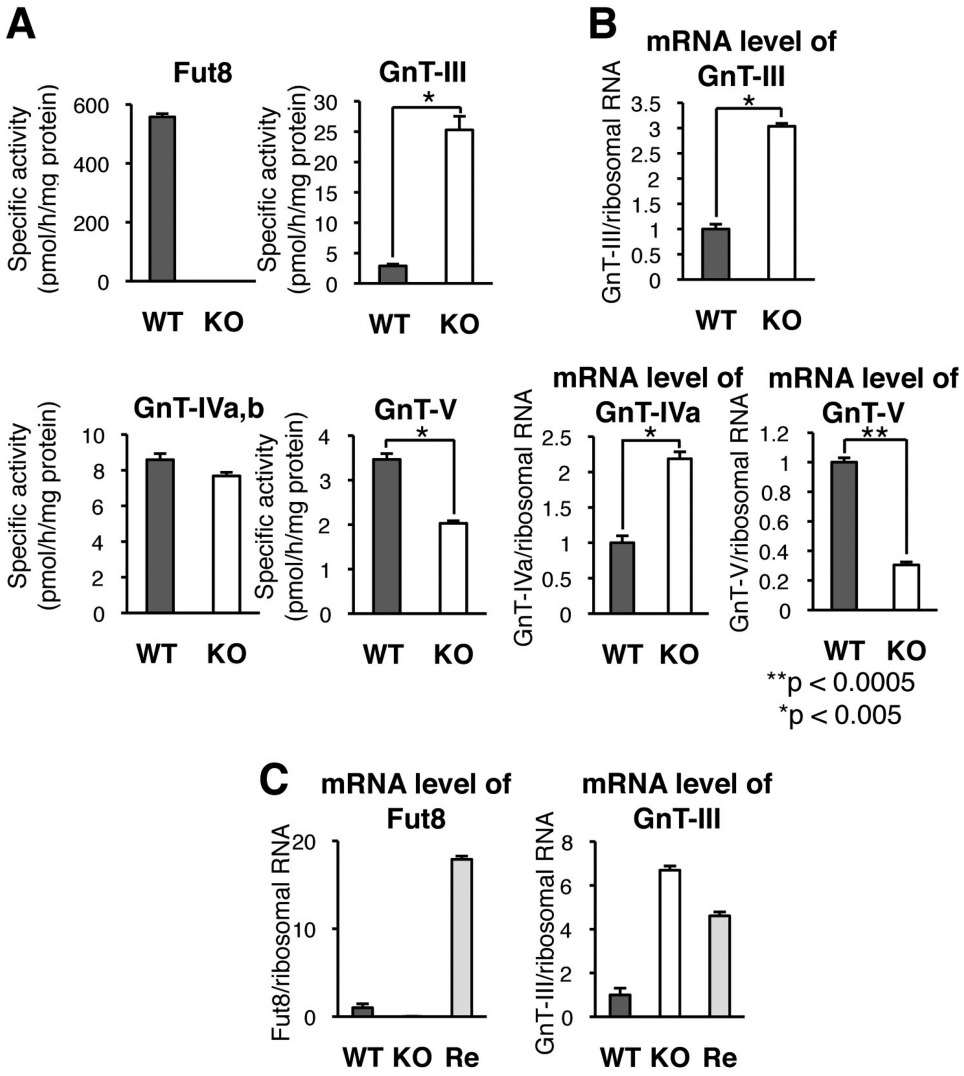

FIGURE 2. **The activity and expression level of GnT-III were up-regulated in *Fut8*$^{-/-}$ MEFs.** *A*, Fut8, GnT-III, GnT-IVa,b, and GnT-V enzyme activities in *Fut8*$^{+/+}$ and *Fut8*$^{-/-}$ MEF lysates are shown as the means ± S.E. ($n = 3$) *B*, *Fut8*$^{+/+}$ and *Fut8*$^{-/-}$ MEFs grown on 10-cm dishes were harvested in 100% confluency. Expression levels of GnT-III, -IVa, -V and ribosomal mRNAs in these MEFs were quantified by real-time PCR. The expression levels of GnT-III, -IVa, and -V were normalized by the corresponding ribosomal RNA expression levels. Data are presented as mean ratio ± S.E. ($n = 3$). *C*, expression levels of Fut8, GnT-III, and ribosomal mRNAs in *Fut8*$^{+/+}$, *Fut8*$^{-/-}$ and reintroduced MEFs (*Re*) were quantified by real-time PCR. The expression levels of Fut8 and GnT-III were normalized by the corresponding ribosomal RNA expression levels. Data are presented as the mean ratio ± S.E. ($n = 3$).

Microarray Analysis—Poly(A)+ RNA was isolated from the cells using an mTRAP kit (ACTIVE MOTIF). The quality of RNA was measured using 2100 Bioanalyzer (Agilent). The RNAs were stored at −80 °C until use. Briefly, total RNAs were then reverse-transcribed into cDNA, and biotinylated cDNAs were synthesized using the GeneChip 3′IVT Express kit (Affymetrix). DNA microarray experiments were performed using Mouse Genome 430 v2.0 (Affymetrix). The hybridization signal on the chip was scanned using a GeneChip 3000 7G scanner and processed by GeneChip operating software (GCOS) Ver. 1.4 (Affymetrix). The DNA microarray expression profiles were compared between *Fut8*$^{+/+}$ and *Fut8*$^{-/-}$ MEFs.

Transient Transfection—The MEF cells (2×10^6) were transfected with 3 μg of pcDNA 3.1+/mouse Fut8-FLAG plasmid (or empty vector) using an MEF Nucleofector Kit2 (Lonza), in conjunction with program T-020 of the Amaxa Nucleofector II system. Cells were harvested after reaching 100% confluence.

Quantitative PCR—Total RNAs were isolated from MEFs using TRI Reagent (Molecular Research Center, Inc.) according to the manufacturer's instructions. Three μg of the RNAs was reverse-transcribed with random hexamers using a SuperScript III first-strand synthesis system for RT-PCR (Invitrogen) according to the manufacturer's protocol. The expression levels of the target genes were measured in duplicate and normalized by the corresponding ribosomal RNA expression levels. For real-time quantitative PCR assay, GnT-III, β-catenin, ribosomal RNA primers and probes, Assay-on-Demand gene expression products, and cDNAs were added to TaqMan universal PCR master mix (Applied Biosystems). The probes for GnT-III and β-catenin were labeled with FAM at its 5′-end and with quencher minor groove binder at its 3′-end. The probe for ribosomal RNA was labeled with VIC at its 5′-end and with quencher TAMRA at its 3′-end. The cDNAs were amplified by one cycle at 50 °C for 2 min, one cycle at 95 °C for 10 min, and 40 cycles at 95 °C for 15 s and 60 °C for 1 min in a total volume of 20

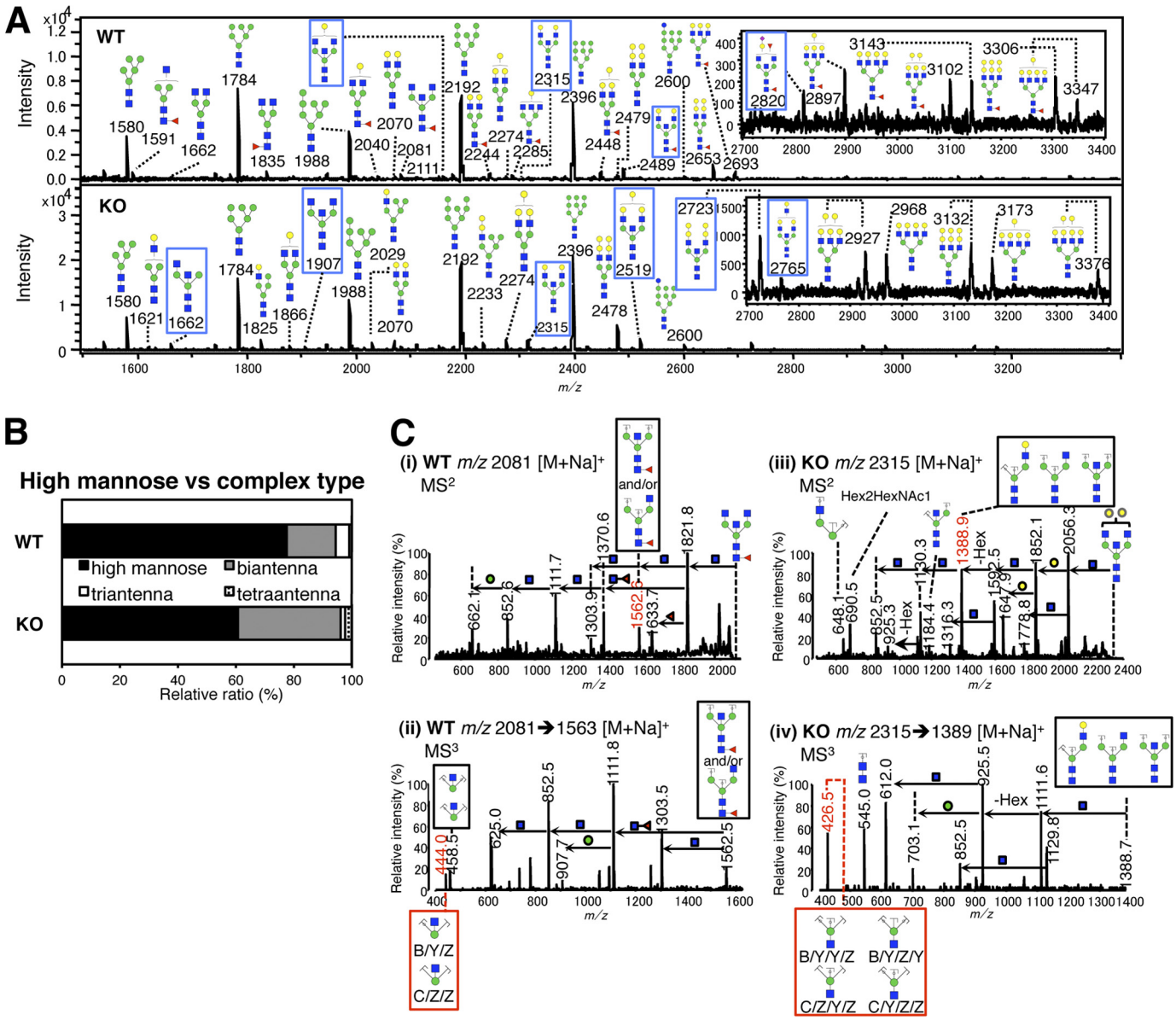

FIGURE 3. **Overall *N*-glycan structural analysis by MALDI-TOF MS.** *A*, MALDI-TOF mass spectra of *N*-linked glycans from *Fut8*$^{+/+}$ and *Fut8*$^{-/-}$ MEFs. Glycan nomenclature and the representation of oligosaccharides are in accordance with the guidelines proposed by the Consortium for Functional Glycomics. All observed ions correspond to $[M + Na]^+$. *B*, glycan prevalence, which is calculated by normalizing the signal intensity of an individual glycan to the summed intensities for all detected glycans (high mannose, bi-, tri-, and tetraantenna complex type glycan), is described as the percentage of total profile. *C*, MS^2 and MS^3 spectra of permethylated *N*-glycans from *Fut8*$^{+/+}$ (*panels i* and *ii*) and *Fut8*$^{-/-}$ MEFs (*panels iii* and *iv*), respectively. The fragment ions at *m/z* 444.0 (*panel ii*) and *m/z* 426.5 (*panel iv*) indicate that precursor ions have a bisecting GlcNAc.

μl using an ABI PRISM 7900HT sequence detection system (Applied Biosystems).

Preparation of a Membrane and Cytosolic Fraction from MEFs—To prepare membrane and cytosolic fractions, MEFs were harvested with 1 ml of PBS containing a protease inhibitor cocktail and homogenized with a potter homogenizer. The obtained homogenates were centrifuged at 100,000 × *g* for 33 min at 4 °C. The supernatant was collected as the cytosolic fraction. The precipitate was resuspended in 1 ml of 1% Triton X-100 in PBS containing a protease inhibitor cocktail followed by rotation at 4 °C overnight and then centrifuged at 100,000 × *g* for 23 min at 4 °C. The supernatant was collected as the membrane fraction. The concentration of protein was determined using a BCA protein assay (Thermo Scientific).

RESULTS

N-Glycan Structures Were Markedly Altered in Fut8$^{-/-}$ *MEFs*—To investigate how loss of core fucosylation affects overall *N*-glycan structures, we carried out a series of lectin blot analyses for MEFs derived from *Fut8*$^{+/+}$ and *Fut8*$^{-/-}$ mice. First, the application of AAL lectin, which preferentially recognizes fucose (32) (Fig. 1*A*), verified the loss of core fucose in lysates of *Fut8*$^{-/-}$ MEFs (Fig. 1*B*, *left*). The bands at 118 and 70 kDa (shown as *asterisk*) in the *Fut8*$^{-/-}$ MEFs were nonspecific bands and were detected by the avidin-horseradish peroxidase conjugate (32). A marked increase in bisecting GlcNAc in the *Fut8*$^{-/-}$ MEFs was detected by E4-PHA blotting (Fig. 1*B*, *middle*). An overall decrease in the signal intensities of L4-PHA, a

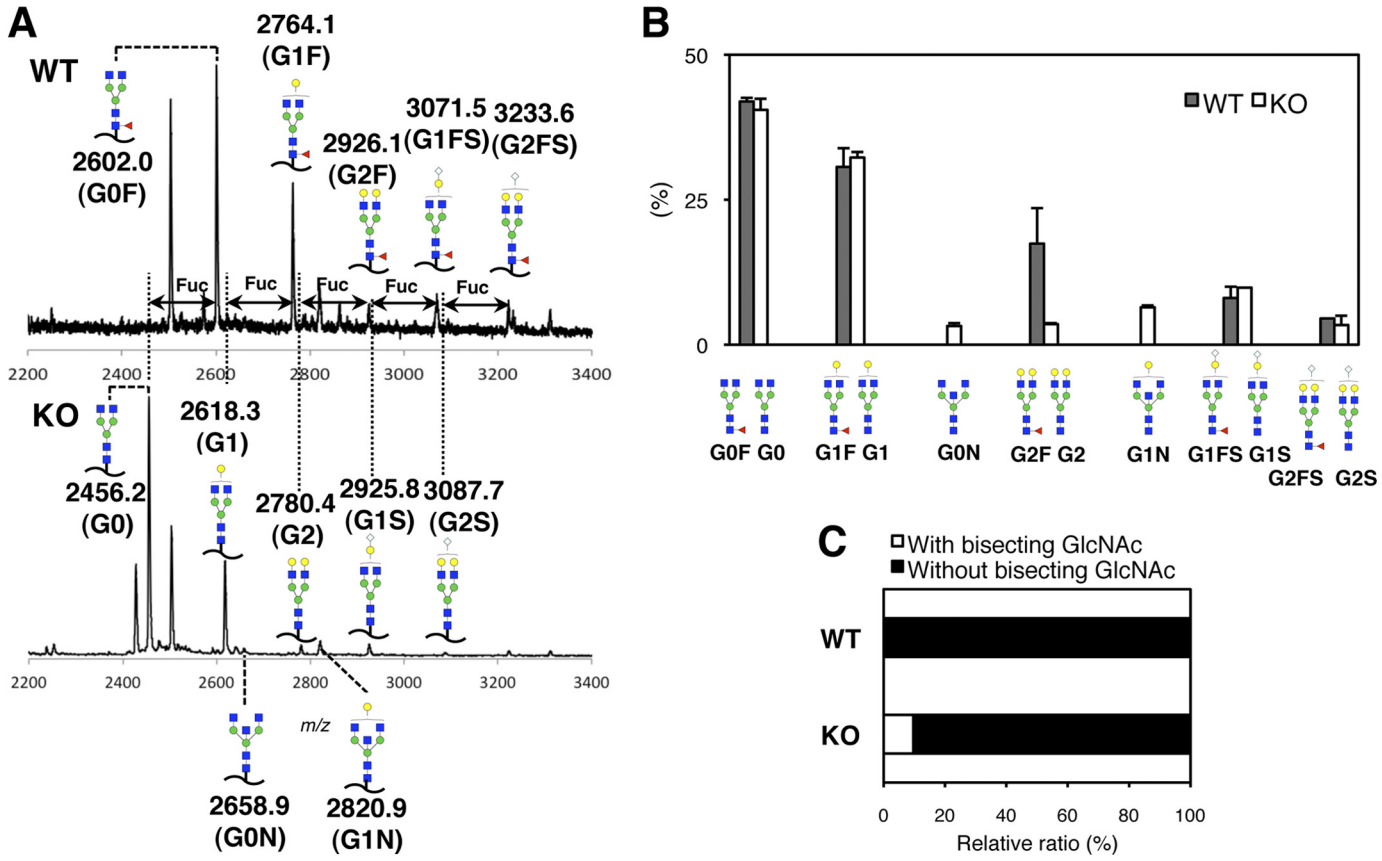

FIGURE 4. **Bisecting GlcNAc containing glycan was observed in IgG_1 only from *Fut8*$^{-/-}$ mouse serum.** *A*, MALDI-TOF mass spectrum of the IgG_1-derived glycopeptides from *Fut8*$^{+/+}$ (*upper panel*) and *Fut8*$^{-/-}$ (*lower panel*) are shown. All of these identified ions were derived from the Asn-297-containing IgG_1 peptide with 1156.5 Da (EEQFNSTFR). *B*, glycopeptide profile derived from of serum IgG_1 of *Fut8*$^{+/+}$ and *Fut8*$^{-/-}$ mice. The data represent the mean ± S.E. (n = 3). *C*, in *Fut8*$^{-/-}$ mice serum, 9.7% of glycan was bisected glycan.

β1,6-GlcNAc branch in *N*-glycan, was observed (Fig. 1*B*, *right*). This could be explained by the fact that GnT-III activity competes with that of a β1,6-GlcNAc branch-synthesizing enzyme GnT-V (33). It should be noted, however, that several exceptionally strong signals were detected with L4-PHA lectin in the lysates of *Fut8*$^{-/-}$ MEFs.

On the assumption that a specific GnT activity would be altered in *Fut8*$^{-/-}$ MEFs, we measured the activities of a series of GnT enzymes (GnT-III, IVa,b, and -V) in *Fut8*$^{+/+}$ and *Fut8*$^{-/-}$ MEFs. We confirmed the complete lack of Fut8 activity in *Fut8*$^{-/-}$ MEFs. We detected a marked increase (~8-fold) in GnT-III activity in *Fut8*$^{-/-}$ MEFs (Fig. 2*A*), although the GnT-V activity in *Fut8*$^{-/-}$ MEFs was decreased to about ~60%. Furthermore, real-time quantitative PCR analysis revealed that GnT-III mRNA was increased by ~3-fold, and the mRNA level of GnT-V was decreased to 30% (Fig. 2*B*), suggesting that the change in glycan structure is controlled at transcription level in GnT-III and -V. The mRNA level of GnT-IVa in *Fut8*$^{-/-}$ was increased 2-fold as compared with those in *Fut8*$^{+/+}$ MEFs. In contrast, the activity of GnT-IVa,b was not altered in *Fut8*$^{-/-}$ MEFs. This can be attributed to the alteration in the mRNA level of GnT-IVb. To address the effects of the expression of Fut8 on expression of GnT-III, we reintroduced the *Fut8* gene into *Fut8*$^{-/-}$ MEFs. As shown in Fig. 2*C*, the mRNA level of GnT-III was down-regulated in the reintroduced MEFs.

These alterations in glycosylation were investigated by a comparative glycomic analysis in which *N*-glycans were enzymatically released from the cell lysates of *Fut8*$^{+/+}$ and *Fut8*$^{-/-}$ MEFs. The resulting free *N*-glycans were then permethylated to facilitate their analysis by MALDI-TOF MS. The acquired mass spectra of the *N*-glycans are shown in Fig. 3*A*. All signals corresponding to mono-fucosylated glycans detected in *Fut8*$^{+/+}$ MEFs completely disappeared in *Fut8*$^{-/-}$ MEFs. As shown in Fig. 3*B*, the relative proportions of the high mannose to total *N*-glycans decreased by ~80% in *Fut8*$^{-/-}$ MEFs as compared with those in *Fut8*$^{+/+}$ MEFs. The relative ratios of bisecting GlcNAc in each branched structure are difficult to compare between WT and KO MEFs. However, as shown in Fig. 3*A*, in WT MEFs bisected biantennary sugar chains were found at *m/z* 2111, 2315, 2489, and 2820, whereas in KO MEFs 1662, 1907, 2315, 2519, 2723, and triantennary sugar chain 2765 were found. All these peaks were assigned by MS^2 or MS^3 analysis.

The structural assignment of bisecting GlcNAc-containing *N*-glycans observed in MS analysis was performed based on subsequent MS/MS analysis data using AXIMA-QIT TOF MS (Fig. 3*C*). The sodiated ion at *m/z* 2081 obtained from *Fut8*$^{+/+}$ MEFs was subjected to MS^2 analysis in Fig. 3*C* (*panel i*). We observed the product ion at *m/z* 444.0 (B/Y/Z and/or C/Z/Z) at MS^3 (Fig. 3*C* (*panel ii*)), which contains the bisecting GlcNAc, produced from the precursor ion at *m/z* 1562.6 (Fuc1Hex3HexNAc3). The precursor ion is composed of two

possible fragments as shown in Fig. 3*C* (*panel i*). The ion at *m/z* 444 is previously reported as a key product ion bearing a bisecting GlcNAc containing glycan (34).

We next performed an MS/MS analysis of the sodiated ion at *m/z* 2315 from *Fut8*$^{-/-}$ MEFs at the MS^2 stage. The ion at *m/z* 1388.9, which is composed of Hex3HexNAc3, consists of three possible isomeric structures (Fig. 3*C* (*panel iii*)). In the *m/z* 1389 fragment in the MS^3 spectra (Fig. 3*C* (*panel iv*)), the ion at *m/z* 426.5 (Man-GlcNAc) was observed, which corresponds to the loss of a branching hexose and bisecting GlcNAc.

IgG$_1$ Derived from Fut8$^{-/-}$ *Mice Serum Contained Increased Bisecting GlcNAc*—Because we anticipated that an increase in bisecting GlcNAc would be also observed *in vivo*, we next performed glycopeptide structural analyses of serum IgG$_1$ derived from *Fut8*$^{+/+}$ and *Fut8*$^{-/-}$ mice using MALDI-TOF MS. We confirmed that all of the IgG$_1$ glycans in *Fut8*$^{-/-}$ mice lacked a core fucose unit (Fig. 4*A*, *lower*), whereas IgG$_1$ glycans obtained from *Fut8*$^{+/+}$ mice were fully modified with core fucose (Fig. 4*A*, *upper*). Mizuochi *et al.* (35) previously reported that most of IgGs from mice were core fucosylated and contained no bisecting GlcNAc. Most of glycopeptides in *Fut8*$^{-/-}$ were non-core fucosylated forms of the structures observed in *Fut8*$^{+/+}$. Therefore, although the ions at *m/z* 2926.1 in *Fut8*$^{+/+}$ and at *m/z* 2925.8 in *Fut8*$^{-/-}$ showed close mass numbers, we assigned the ion at *m/z* 2925.8 in *Fut8*$^{-/-}$ as the non-core fucosylated form of the *m/z* 3071.5 (G1FS) fragment in *Fut8*$^{+/+}$.

The glycan profiles are summarized in Fig. 4*B*. In the case of IgG$_1$ from *Fut8*$^{+/+}$ mice, bisecting GlcNAc was not detectable. In *Fut8*$^{-/-}$ mice, the ratio of simple biantennary glycan (G2) in IgG$_1$ was significantly reduced as compared with its core fucosylated form (G2F) in *Fut8*$^{+/+}$ mice, and a marked increase in bisecting GlcNAc-containing glycans, such as G0N and G1N, was clearly observed. Actually, bisected *N*-glycans were not detectable in IgG$_1$ from *Fut8*$^{+/+}$ mice, whereas 9.7% of the *N*-glycan contained a bisecting GlcNAc in IgG$_1$ from *Fut8*$^{-/-}$ mice (Fig. 4*C*). These data clearly show that the up-regulation of bisecting GlcNAc was also observed in *Fut8*$^{-/-}$ mice.

Change in the Glycosylation of β1-Integrin and N-cadherin—We and others previously reported that there are several target proteins for GnT-III such as integrins and cadherins (12–14). In addition, a recent study reported that integrin-dependent cell migration and intracellular signaling were down-regulated in the absence of core fucose (36). Therefore, we expected that integrin and/or cadherin would be a target for core fucose/bisecting GlcNAc and contain an increased level of bisecting *N*-glycan in *Fut8*$^{-/-}$ MEFs. Western blot analysis of the immunoprecipitated β1-integrin from both *Fut8*$^{+/+}$ and *Fut8*$^{-/-}$ MEFs showed double bands, and the upper band of β1-integin, corresponding to the mature form, migrated faster in *Fut8*$^{-/-}$ MEFs (Fig. 5*A*, *upper*). This difference was not cancelled by sialidase treatment (Fig. 5*B*), indicating that the glycan structure of the β1-integrin other than sialylation constitutes the difference between *Fut8*$^{+/+}$ and *Fut8*$^{-/-}$ MEFs. Lectin blot analysis with AAL and E4-PHA showed that the upper band of β1-integrin (from *Fut8*$^{-/-}$ MEFs) lacks core fucose and has a higher level of bisecting GlcNAc (Fig. 5*A*, *lower*). We unexpectedly observed a marked increase in the L4-PHA epitope on β1-integrin, suggesting that the competition of GnT-III and

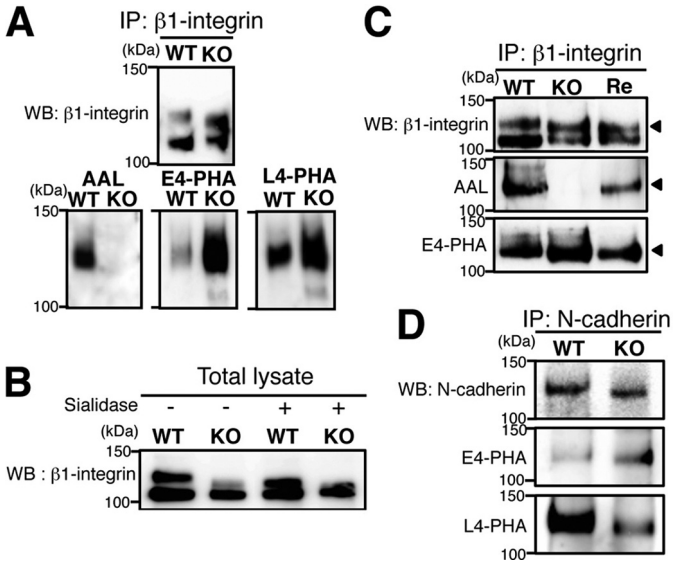

FIGURE 5. **Lectin analysis revealed that glycosylation of β1-integrin and N-cadherin were different between *Fut8*$^{+/+}$ and *Fut8*$^{-/-}$ MEFs.** *A*, immunoprecipitated (*IP*) β1-integrin from *Fut8*$^{+/+}$ and *Fut8*$^{-/-}$ MEF lysates was detected by anti β1-integrin antibody and AAL, E4-PHA, and L4-PHA lectins. *WB*, Western blot. *B*, MEF lysates, with or without sialidase treatment, were subjected to Western blotting with an anti-β1-integrin antibody. The glycan structure of β1-integrin rather than sialylation is different between *Fut8*$^{+/+}$ and *Fut8*$^{-/-}$ MEFs. *C*, lectin blot (AAL and E4-PHA) and Western blotting analyses of immunoprecipitated β1-integrin from *Fut8*$^{+/+}$, *Fut8*$^{-/-}$, and reintroduced (*Re*) MEFs were performed. The upper band of β1-integrin (*arrowhead*) corresponds to the mature form, which is recognized with AAL and E4-PHA. *D*, immunoprecipitated N-cadherin in membrane fractions from *Fut8*$^{+/+}$ and *Fut8*$^{-/-}$ MEFs were detected by anti-N-cadherin antibody and E4-PHA and L4-PHA lectins.

GnT-V is somehow dependent on the type of glycoprotein, although GnT-III and GnT-V compete with each other for the common substrate (37, 38). In the Fut8-reintroduced MEFs, the AAL signal was recovered in the upper band of β1-integrin (Fig. 5*C*, *middle*). The E4-PHA signal on β1-integrin from Fut8-reintroduced MEFs was reduced as compared with *Fut8*$^{-/-}$ MEFs (Fig. 5*C*, *lower*). These results are consistent with the mRNA levels of GnT-III (Fig. 2*C*, *right*).

Because a major cadherin component in MEFs is N-cadherin instead of E-cadherin (39), glycosylation status of N-cadherin was examined in both types of cells (Fig. 5*D*). We found enhanced E4-PHA signals and reduced L4-PHA in the immunoprecipitated N-cadherin from *Fut8*$^{-/-}$ MEFs. These data show that β1-integrin and N-cadherin are highly modified with bisecting GlcNAc by the lack of their core fucose.

Increase in β-Catenin Levels and Down-regulation of Phosphorylation—Our data showed that the absence of core fucose up-regulates bisecting GlcNAc level through increased expression of GnT-III gene. To explore the underlying mechanism of GnT-III gene up-regulation, we carried out DNA microarray analysis of *Fut8*$^{+/+}$ and *Fut8*$^{-/-}$ MEFs. We found that Wnt-responsive genes were significantly up-regulated in *Fut8*$^{-/-}$ MEFs, including the growth arrest-specific 1 gene (12.1-fold increase) and the Frizzled homolog 6 gene (2.3-fold increase) (Table 1), suggesting that Wnt/β-catenin signaling is enhanced in *Fut8*$^{-/-}$ MEFs. In fact, the level of β-catenin was increased in *Fut8*$^{-/-}$ MEFs in terms of protein content as well as mRNA levels as judged by real-time quantitative PCR and

Western blotting (Fig. 6, *A* and *C*). The degradation of β-catenin by the proteasome strictly depends upon its phosphorylation status (40). To determine the phosphorylation level of β-catenin, we carried out Western blotting, the results of which indicated that the phosphorylation level of β-catenin was decreased (Fig. 6*B*) in *Fut8*$^{-/-}$ MEFs. The result suggests that the N-cadherin-β-catenin complex is not sufficiently degraded by the ubiquitin/proteasome pathway and accumulates in the cytosol and nuclei (Fig. 6*C*), although N-cadherin/β-catenin complex level was not changed (Fig. 6*D*).

TABLE 1

Gene expression analysis by a DNA microarray

Fut8$^{+/+}$ and *Fut8*$^{-/-}$ MEFs grown on 15-cm dishes were harvested in 100% confluency. Wnt-related genes that changed expression significantly ($p < 0.00005$) in *Fut8*$^{-/-}$ MEFs as compared with those in *Fut8*$^{+/+}$ MEFs were listed.

Gene name	Fut8 KO/WT -fold change
Wnt target	
Growth arrest-specific 1 (GAS1)	12.1
Frizzled homolog 6 (FZD6)	2.30
Glutathione *S*-transferase, μ type1 (GSTM1)	11.3
Cytochrome P450, family 1, subfamily B, polypeptide1 (CYP1B1)	9.84
Mitochondrial aldehyde dehydrogenase 2 (ALDH2)	2.82
Oxidative stress	
Holocytochrome *c* synthetase (HCCS)	2.64
Glutathione S-transferase, μ type5 (GSTM5)	2.46
Squalene epoxidase (SQLE)	2.46
Nuclear factor, erythroid-derived 2, like 2 (Nfe2l2)(Nrf2)	2.00

Wnt Signal Inhibitor (IWP-2) Reduced mRNA Level of GnT-III in MEFs—We speculated that enhanced Wnt/β-catenin signaling contributed to the up-regulation of GnT-III gene. To confirm whether or not Wnt signaling is involved in the up-regulation of GnT-III, IWP-2, an inhibitor of the *O*-acyltransferase, porcupine, which palmitoylates Wnt, was added to the culture medium, and the level of GnT-III was determined. Indeed, IWP-2 decreased the mRNA levels of β-catenin to 67% of the control in *Fut8*$^{-/-}$ MEFs (Fig. 6, *A* and *C*). In addition, expression level of GnT-III was also suppressed to 70% of the mock sample in *Fut8*$^{-/-}$ MEFs, whereas IWP-2 treatment did not have an effect on GnT-V expression (Fig. 6*A*). This suggests that the change in the Wnt/β-catenin signal is highly associated with the up-regulation of GnT-III. Because we also found the reduction of GnT-III expression in *Fut8*$^{+/+}$ MEFs, Wnt signaling pathway generally up-regulates the GnT-III expression.

DISCUSSION

In this study, our glycomic analysis using glycans released from whole lysates of *Fut8*$^{+/+}$ and *Fut8*$^{-/-}$ MEFs revealed an

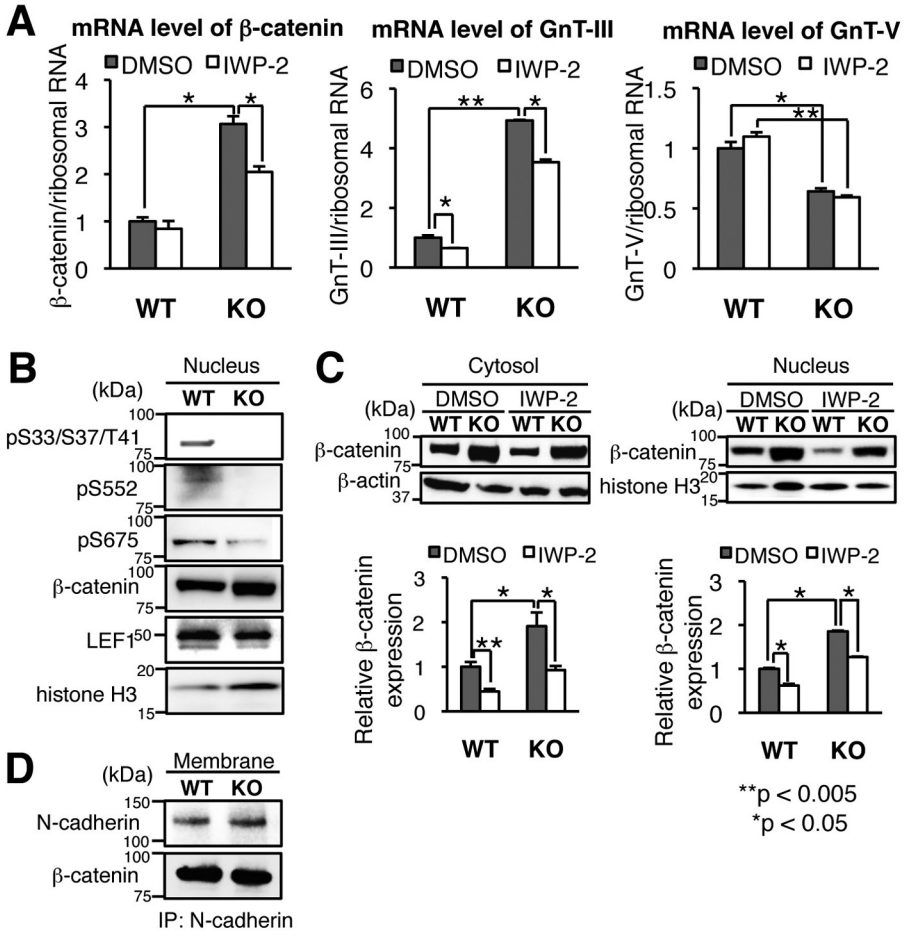

FIGURE 6. **Inhibition of Wnt signal induced down-regulation of mRNA levels of β-catenin and GnT-III in *Fut8*$^{-/-}$ MEFs.** *A*, a Wnt signal inhibitor (15 μM IWP-2) significantly reduced the mRNA levels of β-catenin and GnT-III. In contrast, the mRNA levels of GnT-V were not altered when the MEFs were cultured with 15 μM IWP-2 in *Fut8*$^{+/+}$ and *Fut8*$^{-/-}$. The data represent the mean ± S.E. ($n = 3$). *B*, the phosphorylated β-catenin was down-regulated in *Fut8*$^{-/-}$ MEFs. *pS33/S37/T41*, phospho-Ser-33/Ser-37/Thr-41; *pS552*, phospho-Ser-552; *pS675*, phospho-Ser-675. *IP*, immunoprecipitation. *C*, Wnt signal inhibitor reduced the accumulation of β-catenin in cytosol and nucleus. *D*, coimmunoprecipitation of β-catenin with N-cadherin in *Fut8*$^{+/+}$ and *Fut8*$^{-/-}$ MEFs.

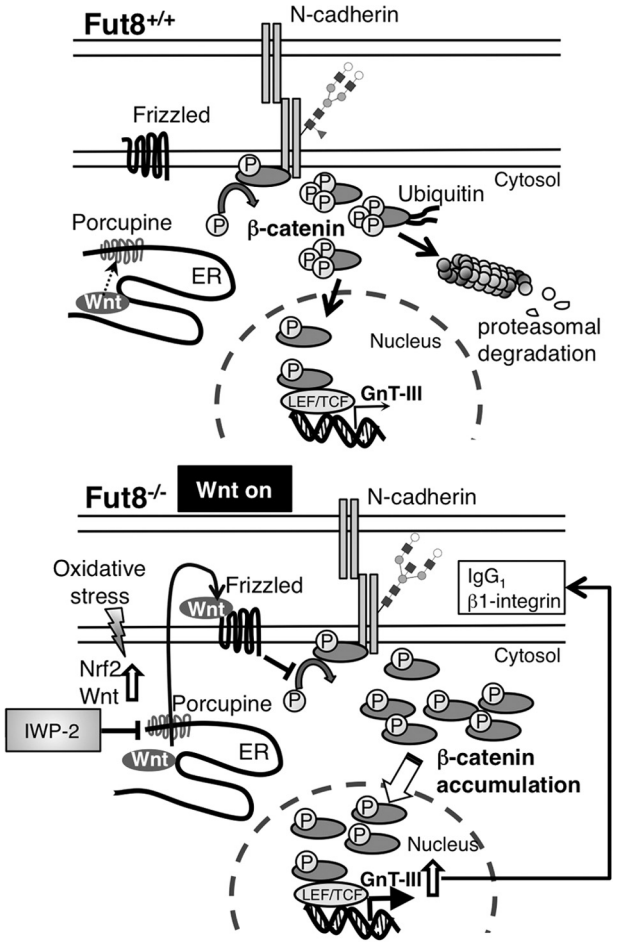

FIGURE 7. **Schematic representation of Wnt signal transduction cascade in *Fut8*$^{+/+}$ and *Fut8*$^{-/-}$ MEFs.** The Wnt is secreted from endoplasmic reticulum (*ER*) by adding palmitoylation by membrane-bound enzyme, *and O*-acyltransferase is designated as porcupine (Wnt on). When the secreted Wnt binds to Frizzled receptor, β-catenin phosphorylation is suppressed, and β-catenin is accumulated in the cytosol and then increased recruitment to nuclei occurs. This may cause the increased expression of GnT-III. In the case of IWP-2, an inhibitor against Wnt signaling or in *Fut8*$^{+/+}$ MEFs, β-catenin secretion to the extracellular space is suppressed, and phosphorylation and ubiquitination are properly processed. Intracellular β-catenin concentration is decreased, and its nuclear recruitment is also decreased. This resulted in the suppression of GnT-III gene expression.

increase in bisected *N*-glycans in *Fut8*$^{-/-}$ MEFs. These data prompted us to investigate whether or not some kinds of compensation for or redundancy of glycan functions may exist in these mice due to the absence of core fucose. We then found a significant increase in bisected *N*-glycan content in *Fut8*$^{-/-}$ MEFs, and that appears to be due to a markedly higher expression of GnT-III mRNA in *Fut8*$^{-/-}$ MEFs. In the case of *Fut8*$^{-/-}$ MEFs, to which Fut8 was reintroduced, the mRNA level of GnT-III was down-regulated, confirming that the expression of Fut8 affects the expression of GnT-III. Microarray analysis with *Fut8*$^{+/+}$ and *Fut8*$^{-/-}$ cells revealed the up-regulation of Wnt target genes. It should be noted that Wnt inhibitor IWP-2, which prevents Wnt secretion, leading to the reduction of cellular level of β-catenin, abrogates GnT-III expression especially in *Fut8*$^{-/-}$ cells. This transcriptional regulation may play a key role in the adaptive response to the loss of core fucose. A recent study by Chen *et al.* (41) shows that Fut8 expression is up-regulated during epithelial-mesenchymal transition, a critical process for malignant transformation of tumor, in the β-catenin/LEF-1-dependent pathway (41). It is interesting that both GnT-III expression and Fut8 expression were regulated by β-catenin/LEF1 pathway.

It is known that E-cadherin/β-catenin-dependent cell-cell adhesion induces GnT-III expression (42). We also found that N-cadherin instead of E-cadherin is expressed in MEFs, but the levels of N-cadherin as well as the N-cadherin-β-catenin complex were comparable in the two types of cells, regardless of the increase in bisected *N*-glycans in N-cadherin from *Fut8*$^{-/-}$ MEFs (Figs. 5*D* and 6*D*). In a microarray analysis, expression of a number of genes other than Wnt target genes was altered by Fut8 deficiency, which might partly explain the adaptive response of *Fut8*$^{-/-}$ mice. In the microarray analysis, we were not able to detect any up-regulation in GnT-III, probably because glycosyltransferase expression, including that for GnT-III, is too low to permit a satisfactory quantitative measurement to be made, as reported previously (43, 44).

In *Fut8*$^{-/-}$ MEFs as well as in *Fut8*$^{-/-}$ mice, the absence of core fucose induces oxidative stress as judged by up-regulation of various oxidative stress-related genes including a major transcription factor Nrf2 (Table 1). Funato *et al.* (45) show that oxidative stress induces up-regulation of Wnt target genes. This suggests that deficiency in Fut8 might cause oxidative stress and that up-regulation of GnT-III might be a response to reduce cellular oxidative stress. In fact in *Fut8*$^{-/-}$ mice, 70% of the mice die within 3 days after birth but ~30% survive, suggesting that an adaptive response may have occurred. Adaptive regulation may proceed in some cases of glycosyltransferase KO mice as reported (46–48).

As depicted in Fig. 7, in the case of *Fut8*$^{-/-}$ MEFs, the "Wnt on" situation occurs under oxidative stress conditions. Nrf2 and Wnt are up-regulated, and phosphorylation of β-catenin is inhibited. β-Catenin was then accumulated in cytosol and nuclei and cooperated with LEF1 to activate GnT-III gene.

This study may open a new insight into the elucidation of adaptive response *in vivo* in terms of glycan functions. Clarification of such compensation or redundancy mechanism would reveal how glycan functions are maintained *in vivo*.

REFERENCES

1. Orr, S. L., Le, D., Long, J. M., Sobieszczuk, P., Ma, B., Tian, H., Fang, X., Paulson, J. C., Marth, J. D., and Varki, N. (2013) A phenotype survey of 36 mutant mouse strains with gene-targeted defects in glycosyltransferases or glycan-binding proteins. *Glycobiology* **23,** 363–380
2. Wilson, J. R., Williams, D., and Schachter, H. (1976) The control of glycoprotein synthesis: *N*-acetylglucosamine linkage to a mannose residue as a signal for the attachment of L-fucose to the asparagine-linked *N*-acetylglucosamine residue of glycopeptide from α1-acid glycoprotein. *Biochem. Biophys. Res. Commun.* **72,** 909–916
3. Uozumi, N., Yanagidani, S., Miyoshi, E., Ihara, Y., Sakuma, T., Gao, C. X., Teshima, T., Fujii, S., Shiba, T., and Taniguchi, N. (1996) Purification and cDNA cloning of porcine brain GDP-L-Fuc:*N*-acetyl-β-D-glucosaminide α1→6fucosyltransferase. *J. Biol. Chem.* **271,** 27810–27817
4. Yanagidani, S., Uozumi, N., Ihara, Y., Miyoshi, E., Yamaguchi, N., and Taniguchi, N. (1997) Purification and cDNA cloning of GDP-L-Fuc:*N*-acetyl-β-D-glucosaminide:α1–6 fucosyltransferase (α1–6 FucT) from human gastric cancer MKN45 cells. *J. Biochem.* **121,** 626–632
5. Wang, X., Inoue, S., Gu, J., Miyoshi, E., Noda, K., Li, W., Mizuno-Horikawa, Y., Nakano, M., Asahi, M., Takahashi, M., Uozumi, N., Ihara, S., Lee, S. H., Ikeda, Y., Yamaguchi, Y., Aze, Y., Tomiyama, Y., Fujii, J., Suzuki,

K., Kondo, A., Shapiro, S. D., Lopez-Otin, C., Kuwaki, T., Okabe, M., Honke, K., and Taniguchi, N. (2005) Dysregulation of TGF-β1 receptor activation leads to abnormal lung development and emphysema-like phenotype in core fucose-deficient mice. *Proc. Natl. Acad. Sci. U.S.A.* **102,** 15791–15796

6. Wang, X., Gu, J., Ihara, H., Miyoshi, E., Honke, K., and Taniguchi, N. (2006) Core fucosylation regulates epidermal growth factor receptor-mediated intracellular signaling. *J. Biol. Chem.* **281,** 2572–2577
7. Wang, X., Gu, J., Miyoshi, E., Honke, K., and Taniguchi, N. (2006) Phenotype changes of Fut8 knockout mouse: core fucosylation is crucial for the function of growth factor receptor(s). *Methods Enzymol.* **417,** 11–22
8. Shinkawa, T., Nakamura, K., Yamane, N., Shoji-Hosaka, E., Kanda, Y., Sakurada, M., Uchida, K., Anazawa, H., Satoh, M., Yamasaki, M., Hanai, N., and Shitara, K. (2003) The absence of fucose but not the presence of galactose or bisecting *N*-acetylglucosamine of human IgG1 complex-type oligosaccharides shows the critical role of enhancing antibody-dependent cellular cytotoxicity. *J. Biol. Chem.* **278,** 3466–3473
9. Matsumiya, S., Yamaguchi, Y., Saito, J., Nagano, M., Sasakawa, H., Otaki, S., Satoh, M., Shitara, K., and Kato, K. (2007) Structural comparison of fucosylated and nonfucosylated Fc fragments of human immunoglobulin G1. *J. Mol. Biol.* **368,** 767–779
10. Umaña, P., Jean-Mairet, J., Moudry, R., Amstutz, H., and Bailey, J. E. (1999) Engineered glycoforms of an antineuroblastoma IgG1 with optimized antibody-dependent cellular cytotoxic activity. *Nat. Biotechnol.* **17,** 176–180
11. Hodoniczky, J., Zheng, Y. Z., and James, D. C. (2005) Control of recombinant monoclonal antibody effector functions by Fc *N*-glycan remodeling *in vitro*. *Biotechnol. Prog.* **21,** 1644–1652
12. Xu, Q., Isaji, T., Lu, Y., Gu, W., Kondo, M., Fukuda, T., Du, Y., and Gu, J. (2012) Roles of *N*-acetylglucosaminyltransferase III in epithelial-to-mesenchymal transition induced by transforming growth factor β1 (TGF-β1) in epithelial cell lines. *J. Biol. Chem.* **287,** 16563–16574
13. Kitada, T., Miyoshi, E., Noda, K., Higashiyama, S., Ihara, H., Matsuura, N., Hayashi, N., Kawata, S., Matsuzawa, Y., and Taniguchi, N. (2001) The addition of bisecting *N*-acetylglucosamine residues to E-cadherin down-regulates the tyrosine phosphorylation of β-catenin. *J. Biol. Chem.* **276,** 475–480
14. Shigeta, M., Shibukawa, Y., Ihara, H., Miyoshi, E., Taniguchi, N., and Gu, J. (2006) β1,4-*N*-Acetylglucosaminyltransferase III potentiates β1 integrin-mediated neuritogenesis induced by serum deprivation in Neuro2a cells. *Glycobiology* **16,** 564–571
15. Yoshimura, M., Ihara, Y., Matsuzawa, Y., and Taniguchi, N. (1996) Aberrant glycosylation of E-cadherin enhances cell-cell binding to suppress metastasis. *J. Biol. Chem.* **271,** 13811–13815
16. Pinho, S. S., Figueiredo, J., Cabral, J., Carvalho, S., Dourado, J., Magalhães, A., Gärtner, F., Mendonfa, A. M., Isaji, T., Gu, J., Carneiro, F., Seruca, R., Taniguchi, N., and Reis, C. A. (2013) E-cadherin and adherens-junctions stability in gastric carcinoma: functional implications of glycosyltransferases involving *N*-glycan branching biosynthesis, *N*-acetylglucosaminyltransferases III and V. *Biochim. Biophys. Acta* **1830,** 2690–2700
17. Pinho, S. S., Reis, C. A., Paredes, J., Magalhães, A. M., Ferreira, A. C., Figueiredo, J., Xiaogang, W., Carneiro, F., Gärtner, F., and Seruca, R. (2009) The role of *N*-acetylglucosaminyltransferase III and V in the post-transcriptional modifications of E-cadherin. *Hum. Mol. Genet.* **18,** 2599–2608
18. Takahashi, M., Kuroki, Y., Ohtsubo, K., and Taniguchi, N. (2009) Core fucose and bisecting GlcNAc, the direct modifiers of the *N*-glycan core: their functions and target proteins. *Carbohydr. Res.* **344,** 1387–1390
19. Taniguchi, N., Miyoshi, E., Gu, J., Jianguo, G., Honke, K., and Matsumoto, A. (2006) Decoding sugar functions by identifying target glycoproteins. *Curr. Opin. Struct. Biol.* **16,** 561–566
20. Taniguchi, N., Yoshimura, M., Miyoshi, E., Ihara, Y., Nishikawa, A., and Fujii, S. (1996) Remodeling of cell surface glycoproteins by *N*-acetylglucosaminyltransferase III gene transfection: modulation of metastatic potentials and down regulation of hepatitis B virus replication. *Glycobiology* **6,** 691–694
21. Santer, U. V., and Glick, M. C. (1979) Partial structure of a membrane glycopeptide from virus-transformed hamster cells. *Biochemistry* **18,** 2533–2540
22. Longmore, G. D., and Schachter, H. (1982) Product-identification and substrate-specificity studies of the GDP-L-fucose:2-acetamido-2-deoxy-β-D-glucoside (FUC goes to Asn-linked GlcNAc) 6-α-L-fucosyltransferase in a Golgi-rich fraction from porcine liver. *Carbohydr. Res.* **100,** 365–392
23. Nishima, W., Miyashita, N., Yamaguchi, Y., Sugita, Y., and Re, S. (2012) Effect of bisecting GlcNAc and core fucosylation on conformational properties of biantennary complex-type *N*-glycans in solution. *J. Phys. Chem. B* **116,** 8504–8512
24. Korekane, H., Matsumoto, A., Ota, F., Hasegawa, T., Misonou, Y., Shida, K., Miyamoto, Y., and Taniguchi, N. (2010) Involvement of ST6Gal I in the biosynthesis of a unique human colon cancer biomarker candidate, α2,6-sialylated blood group type 2H (ST2H) antigen. *J. Biochem.* **148,** 359–370
25. Nishikawa, A., Gu, J., Fujii, S., and Taniguchi, N. (1990) Determination of *N*-acetylglucosaminyltransferases III, IV and V in normal and hepatoma tissues of rats. *Biochim. Biophys. Acta* **1035,** 313–318
26. Hodge, J. E., and Hofreiter, B. T. (1962) Determination of reducing sugars and carbohydrates in *Methods Carbohydr. Chem.* (Whistler, R. L. and Wolfrom, J. L., eds) Vol. 1, pp. 380–394, Academic Press, New York
27. Ito, H., Kuno, A., Sawaki, H., Sogabe, M., Ozaki, H., Tanaka, Y., Mizokami, M., Shoda, J., Angata, T., Sato, T., Hirabayashi, J., Ikehara, Y., and Narimatsu, H. (2009) Strategy for glycoproteomics: identification of glycoalteration using multiple glycan profiling tools. *J. Proteome Res.* **8,** 1358–1367
28. Domon, B., and Costello, C. E. (1988) Structure elucidation of glycosphingolipids and gangliosides using high-performance tandem mass spectrometry. *Biochemistry* **27,** 1534–1543
29. Wada, Y., Tajiri, M., and Ohshima, S. (2010) Quantitation of saccharide compositions of *O*-glycans by mass spectrometry of glycopeptides and its application to rheumatoid arthritis. *J. Proteome Res.* **9,** 1367–1373
30. Wada, Y., Tajiri, M., and Yoshida, S. (2004) Hydrophilic affinity isolation and MALDI multiple-stage tandem mass spectrometry of glycopeptides for glycoproteomics. *Anal. Chem.* **76,** 6560–6565
31. Wada, Y., Azadi, P., Costello, C. E., Dell, A., Dwek, R. A., Geyer, H., Geyer, R., Kakehi, K., Karlsson, N. G., Kato, K., Kawasaki, N., Khoo, K. H., Kim, S., Kondo, A., Lattova, E., Mechref, Y., Miyoshi, E., Nakamura, K., Narimatsu, H., Novotny, M. V., Packer, N. H., Perreault, H., Peter-Katalinic, J., Pohlentz, G., Reinhold, V. N., Rudd, P. M., Suzuki, A., and Taniguchi, N. (2007) Comparison of the methods for profiling glycoprotein glycans—HUPO Human Disease Glycomics/Proteome Initiative multi-institutional study. *Glycobiology* **17,** 411–422
32. Matsumura, K., Higashida, K., Ishida, H., Hata, Y., Yamamoto, K., Shigeta, M., Mizuno-Horikawa, Y., Wang, X., Miyoshi, E., Gu, J., and Taniguchi, N. (2007) Carbohydrate binding specificity of a fucose-specific lectin from Aspergillus oryzae: a novel probe for core fucose. *J. Biol. Chem.* **282,** 15700–15708
33. Zhao, Y., Nakagawa, T., Itoh, S., Inamori, K., Isaji, T., Kariya, Y., Kondo, A., Miyoshi, E., Miyazaki, K., Kawasaki, N., Taniguchi, N., and Gu, J. (2006) *N*-Acetylglucosaminyltransferase III antagonizes the effect of *N*-acetylglucosaminyltransferase V on α3β1 integrin-mediated cell migration. *J. Biol. Chem.* **281,** 32122–32130
34. Ashline, D. J., Lapadula, A. J., Liu, Y. H., Lin, M., Grace, M., Pramanik, B., and Reinhold, V. N. (2007) Carbohydrate structural isomers analyzed by sequential mass spectrometry. *Anal. Chem.* **79,** 3830–3842
35. Mizuochi, T., Hamako, J., and Titani, K. (1987) Structures of the sugar chains of mouse immunoglobulin G. *Arch. Biochem. Biophys.* **257,** 387–394
36. Zhao, Y., Itoh, S., Wang, X., Isaji, T., Miyoshi, E., Kariya, Y., Miyazaki, K., Kawasaki, N., Taniguchi, N., and Gu, J. (2006) Deletion of core fucosylation on α3β1 integrin down-regulates its functions. *J. Biol. Chem.* **281,** 38343–38350
37. Schachter, H. (1986) Biosynthetic controls that determine the branching and microheterogeneity of protein-bound oligosaccharides. *Biochem. Cell Biol.* **64,** 163–181
38. Gu, J., Nishikawa, A., Tsuruoka, N., Ohno, M., Yamaguchi, N., Kangawa, K., and Taniguchi, N. (1993) Purification and characterization of UDP-*N*-acetylglucosamine: α-6-D-mannoside β1–6*N*-acetylglucosaminyltransferase (*N*-acetylglucosaminyltransferase V) from a human lung cancer cell line.

J. Biochem. **113,** 614–619
39. Reiss, K., Maretzky, T., Ludwig, A., Tousseyn, T., de Strooper, B., Hartmann, D., and Saftig, P. (2005) ADAM10 cleavage of N-cadherin and regulation of cell-cell adhesion and β-catenin nuclear signalling. *EMBO J.* **24,** 742–752
40. Liu, C., Li, Y., Semenov, M., Han, C., Baeg, G. H., Tan, Y., Zhang, Z., Lin, X., and He, X. (2002) Control of β-catenin phosphorylation/degradation by a dual-kinase mechanism. *Cell* **108,** 837–847
41. Chen, C. Y., Jan, Y. H., Juan, Y. H., Yang, C. J., Huang, M. S., Yu, C. J., Yang, P. C., Hsiao, M., Hsu, T. L., and Wong, C. H. (2013) Fucosyltransferase 8 as a functional regulator of nonsmall cell lung cancer. *Proc. Natl. Acad. Sci. U.S.A.* **110,** 630–635
42. Iijima, J., Zhao, Y., Isaji, T., Kameyama, A., Nakaya, S., Wang, X., Ihara, H., Cheng, X., Nakagawa, T., Miyoshi, E., Kondo, A., Narimatsu, H., Taniguchi, N., and Gu, J. (2006) Cell-cell interaction-dependent regulation of *N*-acetylglucosaminyltransferase III and the bisected *N*-glycans in GE11 epithelial cells. Involvement of E-cadherin-mediated cell adhesion. *J. Biol. Chem.* **281,** 13038–13046
43. Nairn, A. V., York, W. S., Harris, K., Hall, E. M., Pierce, J. M., and Moremen, K. W. (2008) Regulation of glycan structures in animal tissues: transcript profiling of glycan-related genes. *J. Biol. Chem.* **283,** 17298–17313
44. Naito, Y., Takematsu, H., Koyama, S., Miyake, S., Yamamoto, H., Fujinawa, R., Sugai, M., Okuno, Y., Tsujimoto, G., Yamaji, T., Hashimoto, Y., Itohara, S., Kawasaki, T., Suzuki, A., and Kozutsumi, Y. (2007) Germinal center marker GL7 probes activation-dependent repression of *N*-glycolylneuraminic acid, a sialic acid species involved in the negative modulation of B-cell activation. *Mol. Cell Biol.* **27,** 3008–3022
45. Funato, Y., Michiue, T., Asashima, M., and Miki, H. (2006) The thioredoxin-related redox-regulating protein nucleoredoxin inhibits Wnt-β-catenin signalling through dishevelled. *Nat. Cell Biol.* **8,** 501–508
46. Grewal, P. K., McLaughlan, J. M., Moore, C. J., Browning, C. A., and Hewitt, J. E. (2005) Characterization of the LARGE family of putative glycosyltransferases associated with dystroglycanopathies. *Glycobiology* **15,** 912–923
47. Chui, D., Oh-Eda, M., Liao, Y. F., Panneerselvam, K., Lal, A., Marek, K. W., Freeze, H. H., Moremen, K. W., Fukuda, M. N., and Marth, J. D. (1997) α-Mannosidase-II deficiency results in dyserythropoiesis and unveils an alternate pathway in oligosaccharide biosynthesis. *Cell* **90,** 157–167
48. Takamatsu, S., Antonopoulos, A., Ohtsubo, K., Ditto, D., Chiba, Y., Le, D. T., Morris, H. R., Haslam, S. M., Dell, A., Marth, J. D., and Taniguchi, N. (2010) Physiological and glycomic characterization of *N*-acetylglucosaminyltransferase-IVa and -IVb double deficient mice. *Glycobiology* **20,** 485–497